

# Ultra-intense Laser-Driven Target Normal Sheath Radiation in the Terahertz Region

Z. Jin<sup>1</sup>, H.B. Zhuo<sup>2</sup>, J.H. Shin<sup>1</sup>, N. Yugami<sup>3</sup>, M.Y. Yu<sup>4</sup>, Z.M. Sheng<sup>5</sup>, and R. Kodama<sup>1</sup>

<sup>1</sup>Osaka University, 2-1 Yamada-oka, Suita, Osaka, 565-0871, Japan

<sup>2</sup>College of Science, National University of Defense Technology, Changsha 410073, China

<sup>3</sup>Utsunomiya University, Yoto 7-1-2, Utsunomiya, Tochigi, 321-8585, Japan

<sup>4</sup>Zhejiang University, Hangzhou 310027, China

<sup>5</sup>Shanghai Jiao Tong University, Shanghai 200240, China

**Abstract**—Ultra-intense radiation in the terahertz (THz) regime emitted from the rear side of laser-irradiated solid target is experimentally investigated using a 20 TW fs laser system. The THz radiation emitted in a conical angle around 45 degrees is of radially polarized and has its duration of tens of ps. The waveform, angular distribution, polarization and laser intensity dependence of the observed radiation are in good agreement with those predicted for the radiation from deceleration of >sub-MeV electrons passing through the sheath electric field behind the target.

## I. INTRODUCTION

WE present experimental evidence of THz radiation generated by the target normal sheath radiation (TNSR) mechanism [1, 2]. Intense THz emission from the rear side of the target is observed. The measured temporal waveform, angular distribution, as well as polarization indicate that this THz radiation originates from the energetic electron deceleration in the charge-separation field behind the target, which is known for ion acceleration through target normal sheath acceleration (TNSA). The experimental results show a great enhancement of THz energy and a different waveform, comparing with previous studies, which can be benefited from a higher sheath electron number density.

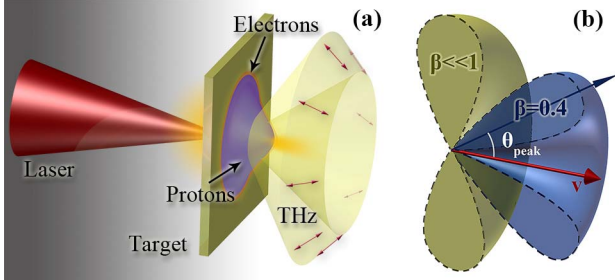


Fig. 1. Schematic of the THz radiation formation process.

Our scheme for generating strong THz radiation is shown in Fig. 1. Relativistic electrons accelerated in laser-solid interaction propagate through the target and establish at its rear a strong charge-separation field or sheath electric field of order  $\sim$ TV/m. The very energetic electrons at the sheath front are decelerated by the intense electrostatic force and thereby emit radiation. The TNSR polarization state, which depends on the directions of the observer and the electron motion, can be assumed to have a radial distribution. The angular power distribution has then a typical relativistic dipole pattern as shown in Fig. 1(b).

## II. RESULTS

The TNSR mechanism is experimentally investigated using the P3 laser facility at Osaka University. The experimental setup is shown in Fig. 2(a). The P3 laser outputs 600 mJ, 800

nm, 30 fs light pulses that are focused on a 10  $\mu$ m -thick copper foil with a peak laser intensity of  $3 \times 10^{19}$  W/cm<sup>2</sup>. The THz radiation from the target's rear side is sent to a single-shot THz time-domain spectroscopy (TDS) system to obtain the temporal wave profile. The single-shot TDS system uses a direct spatial encoding pump-probe electro-optic (EO) sampling scheme [3]. The probe beam, which is reflected by two aluminum echelons to produce 400 (20 $\times$ 20) beamlets at time steps of  $\sim$ 94.3 fs and a total time window of  $\sim$ 37.7 ps, is collinearly focused on a 1 mm-thick  $\langle$ 110 $\rangle$  ZnTe crystal along with the synchronized THz pulse. The THz electric field is encoded with respect to the different positions of the beamlets, which are detected using a 16-bit charge-coupled device (CCD) camera, as shown in Fig. 2(b). The plasma expansion is also monitored using a pump-probe shadowgraph imaging system with 4  $\mu$ m spatial resolution. When the probe beam delay varies from 0 to 100 ps after the arrival of the main laser pulse, expansion of the plasma from the target front surface can be observed, as shown in Fig. 2(c). Due to the slow response of ions, no obvious expansion of the plasma from the target rear surface is observed at this instant, although an intense sheath electric field is formed and sustained by the laser accelerated hot electrons outside the target rear surface, which is crucial for the TNSR generation.

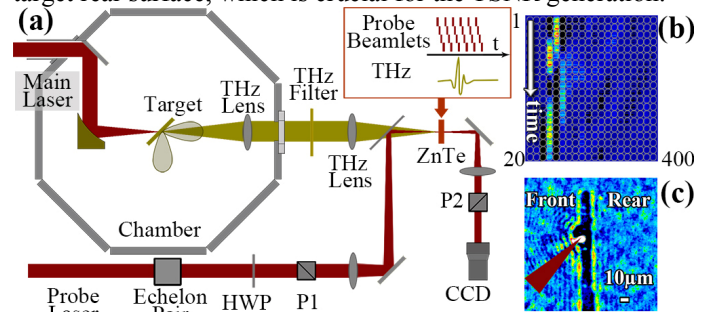
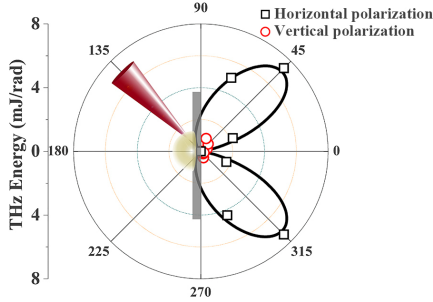


Fig. 2. Experimental setup.

A calibrated Golay cell coupled to a polyethylene THz polarizer is used to measure the THz energy and the polarization. The angular distribution is measured by changing the position of the THz lens inside the chamber. The black squares in Fig. 3 are for the horizontally polarized THz energy ( $E_H$ ), measured in the horizontal plane, and the red circles are for the vertically polarized THz energy ( $E_V$ ), that are close to the noise level. The black solid curve traces the best-fit curve for  $\beta \sim 0.4$ . The angular distribution of the THz energy clearly shows two symmetrical peaks at 45° and 315° to the target normal, and mainly horizontal polarized with  $E_H/E_V > 10$ . To see the three-dimensional characteristics, the radiation in the

vertical plane is also investigated. The THz radiation polarizations are perpendicular ( $E_v/E_H > 10$  at  $45^\circ$ ), but the dipole-like energy distribution pattern is almost identical, to that in the horizontal plane. That is, the measured THz radiation emitted from the target rear surface has a radially symmetric cone structure with radial polarization, agreeing well with the theoretical predictions as shown in Fig. 1(a). The single pulse THz energy measured at  $45^\circ$  is  $\sim 0.35$  mJ with a collection solid angle of 0.0485 sr, corresponding to 7.2 mJ/sr. The total, or integrated, energy emitted into this  $2\pi$  solid angle is at least mJ level, which is much higher than previous reports.



**Fig. 3.** Measured angular distribution of the THz energy in the horizontal plane. The black squares and red circles represent THz energies of horizontal and vertical polarizations, respectively. The black curves are for the best-fit dipole emission pattern.

Figure 4(a) shows the THz radiation profile obtained by the TDS system. The blue and olive-green curves show the THz electric field emitted at  $45^\circ$  from the target normal in the horizontal plane with horizontal and vertical polarizations, respectively. The THz field is mainly horizontally polarized, which is consistent with the results from the Golay cell. In addition to the sub-ps single-cycle oscillation, (as shown in the yellow shaded area), the THz output of TNSR follows with some lower-frequency oscillations, with a width  $\sim 10$  ps, together with high-frequency oscillations that last for more than 30 ps. The long period of this radiation is consistent with the sheath lifetime. Due to adiabatic cooling in the plasma expansion, the sheath electron temperature  $T_e$  drops rapidly to sub MeV within few ps, which implies that the observed THz radiation originates from not only the most energetic electrons at the early time, but also those sub-MeV electrons during the long-time sheath evolution. The inset shows the corresponding spectral distribution.

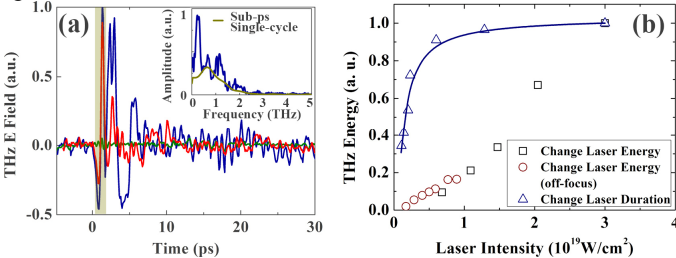


**Fig. 4.** (a) THz waveform, obtained from the single-shot TDS system at  $45^\circ$  from the target normal in the horizontal plane. The blue and olive-green curves are for the THz electric fields of horizontal and vertical polarizations, respectively. The red curve gives the horizontally-polarized THz electric field, when the target is  $\sim 13 \mu\text{m}$  out of the best focus. (b) Dependence of the THz energy to the laser intensity by changing the laser energy (black squares and red circles) and laser duration (blue triangles). The blue solid line is for the fraction of the sheath electrons with energy  $>200$  keV.

Comparing to Ref. 1, enhancement of the THz energy and difference in the waveforms can be attributed to a better

focusing condition. When we shift the target  $\sim 13 \mu\text{m}$  away from the best-focus position, the measured waveform becomes more like a single-cycle field, shows as the red line in Fig. 4(a), similar to that in Ref. 1. Fig. 4(b) gives measured the THz pulse energy when changing the incident laser intensity. The blue triangles give the measured THz energy at the best focus, when changing only the laser pulse duration. The THz energy increase rapidly when the laser intensity is around the relativistic intensity. However, while the intensity is much higher, the THz energy does not increase so much. Taking an assumption of thermal electron energy distribution, the blue solid line gives the fraction of the laser accelerated electrons with energy  $>200$  keV. When the laser intensity is increased to  $\sim 10^{19}$  W/cm $^2$ , the fraction of these electrons is close to 1 and reach to a saturation, which is well consistent with the THz energy measurements.

The black squares and red circles are measured by keeping a same laser duration (30 fs) and changing only the laser energy while target at the best focus position and  $\sim 13 \mu\text{m}$  out of focus, respectively. The THz energy increase linearly with the laser energy density, which is consistent with Ref. 1. While the target is off-focus, the intensity drops to 1/3 and the THz energy drops to 1/7 of the best focus value. Increasing the laser energy or reducing the focus size results in not only a higher electron temperature, but also a higher electron number density and a higher charge separation field. The results indicate that the THz energy strongly depends on the number density of  $>$ sub-MeV sheath electrons, which agrees with the waveform measurements. Furthermore, with a higher charge separation field, the electrons can be confined and oscillating along the sheath for a longer time, which explains the additional oscillations we have observed after the first single-cycle field.

### III. SUMMARY

In summary, intense coherent THz radiation from tabletop laser-solid interaction is experimentally investigated. The wave profile, polarization, and dipole-like pattern of the radiation indicate that it originates from sheath electron deceleration during the TNSA process. And the laser intensity dependence shows that THz yield can be greatly increase with a higher energy, tighter focus laser.

### REFERENCES

- [1]. A. Gopal, S. Herzer, A. Schmidt, P. Singh, A. Reinhard, W. Ziegler, D. Brömmel, A. Karmakar, P. Gibbon, U. Dillner, T. May, H-G. Meyer, and G. G. Paulus, "Observation of Gigawatt-Class THz Pulses from a Compact Laser-Driven Particle Accelerator," *Phys. Rev. Lett.*, vol. 111, pp. 074802, 2013.
- [2]. A. Gopal, P. Singh, S. Herzer, A. Reinhard, A. Schmidt, U. Dillner, T. May, H-G. Meyer, W. Ziegler, and G. G. Paulus, "Characterization of 700  $\mu\text{J}$  T rays generated during high-power laser solid interaction," *Opt. Lett.*, vol. 38, pp. 4705-4707, 2013.
- [3]. K. Y. Kim, B. Yellampalle, A. J. Taylor, G. Rodriguez, and J. H. Glowia, "Single-shot terahertz pulse characterization via two-dimensional electro-optic imaging with dual echelons," *Opt. Lett.*, vol. 32, pp. 1968-1970, 2007.